Synthesis, Spectroscopy, and Hydroformylation Activity of Sterically Demanding, Phosphite-Modified Cobalt Catalysts

by **Reinout Meijboom**[a])[1]), **Marco Haumann**[a])[2]), **Andreas Roodt***[b]), and **Llewellyn Damoense**[a])[c])

[a]) Department of Chemistry, University of Johannesburg, P.O. Box 524, Auckland Park 2006, South Africa
[b]) Department of Chemistry, University of the Free State, P.O. Box 339, Bloemfontein 9300, South Africa (phone: +27-(0)51-4012547; fax: +27-(0)51-4307805; e-mail: roodta.sci@mail.uovs.ac.za)
[c]) *Sasol Technology R&D*, P.O. Box 1, Sasolburg 1947, South Africa

Dedicated to Professor *André E. Merbach* on the occasion of his 65th birthday

The dinuclear complex $[Co_2(CO)_6\{P(O\text{-}2,4\text{-}t\text{-}Bu_2C_6H_3)_3\}_2]$ (**6**) has been synthesised and fully characterised. X-Ray crystal-structure analysis revealed a *trans*-diaxial geometry, no bridging carbonyls, and Co–Co and Co–P bond lengths of 2.706(5) and 2.134(4) Å, respectively. The hydroformylation of pent-1-ene in the presence of **6** was studied at 120–180° at pressures between 20 and 80 bar *Syngas*. High-pressure (HP) spectroscopy (IR, NMR) was used to detect potential hydride intermediates. HP-IR Studies revealed the formation of $[CoH(CO)_3\{P(O\text{-}2,4\text{-}t\text{-}Bu_2C_6H_3)_3\}]$ (**2**) at *ca.* 105°, with no significant amount of $[CoH(CO)_4]$ detectable. The intermediate **2** was synthesised and characterised. The formation of the undesired complex $[CoH(CO)_2\{P(O\text{-}2,4\text{-}t\text{-}Bu_2C_6H_3)_3\}_2]$ was completely suppressed due to the large cone angle of the sterically demanding phosphite.

Introduction. – Discovered in 1938 by *Otto Roelen* at *Ruhrchemie* [1], hydroformylation is, today, the most important application of homogeneous catalysis on an industrial scale [2], with worldwide annual production capacities exceeding 6 million tons. In the hydroformylation reaction, also known as *oxo synthesis*, alkenes react with carbon monoxide (CO) and hydrogen (H_2) in the presence of a transition metal catalyst to form either linear or branched aldehydes.

The first generation of catalysts was based on unmodified $[CoH(CO)_4]$ (**1**), which required high reaction pressures to ensure the stability of the active catalyst and to avoid cobalt plating. In 1966, *Shell* reported a system where the addition of a tertiary phosphine stabilised the catalyst to such an extent that reaction pressures below 100 bar were feasible [3–5]. The larger steric demand of the phosphine ligand, compared to CO, also led to improved selectivity for the desired linear products [6]. However, the activity was low compared to that of the unmodified system. More important from an economic point of view, consecutive hydrogenation of the aldehydes occurred, leading to alcohols as the primary products. This characteristic of the catalyst system can, thus, also result in hydrogenation of the alkene feedstock, leading to eventual undesired alkane formation.

The selectivity can be rationalized by the *Heck–Breslow* mechanism, originally derived for unmodified cobalt catalysis [7]. This mechanism was later generalised and

[1]) Present address: University of the Free State, Bloemfontein.
[2]) Present address: Institut für Chemische Reaktionstechnik, Universität Erlangen-Nürnberg, D-91058 Erlangen.

Scheme 1. *Generalised* Heck – Breslow *Mechanism*

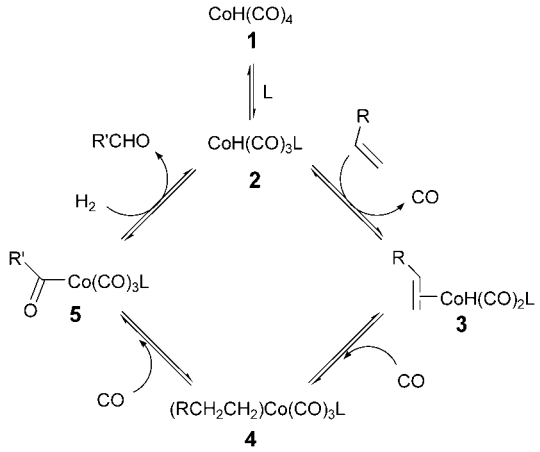

applied to ligand-modified systems as well (*Scheme 1*), in which the catalyst precursor is the monosubstituted hydride, *i.e.*, $[CoH(CO)_3L]$ (**2**).

The unsaturated $[CoH(CO)_2L]$ species **3**, a π-complex, is formed by the loss of a CO ligand and rapid addition of an alkene to the intermediary 16-electron species. Hydrogen transfer to the alkene is influenced by the steric demand of the ligand, leading either to *Markovnikov* or, preferentially, anti-*Markovnikov* addition. In the case of unmodified catalysis, the symmetry of the species should yield equal amounts of linear (l) and branched (b) aldehydes (l/b = 1), and addition of CO produces the alkyl species $[(RCH_2CH_2)Co(CO)_3L]$ (**4**). Alkyl migration to a coordinated CO ligand results in the acyl species $[\{R'C(O)\}Co(CO)_3L]$ (**5**), which is cleaved by H_2 to form the aldehyde, thus regenerating the hydride **2**.

Since the original *Shell* process, based on trialkylphosphines, was introduced, a variety of phosphine ligands have been studied [8]. Recently, the use of tertiary phosphines in which the P-atom is incorporated in a limonene bicycle has been reported [9]. Except for one patent from 1967 [10], no reports on the use of *phosphite* ligands in the Co-catalysed hydroformylation have appeared. Since phosphites should decrease the electron density on the Co centre, relative to phosphines, they are expected to yield fewer hydrogenation products. In a previous publication, we reported triphenylphosphite-modified cobalt hydroformylation studied by high-pressure (HP) NMR, HP-IR, batch autoclave reactions, and independent synthesis of the proposed hydride intermediates [11]. It was found in that study that a large amount of the bis(phosphito)cobalt hydride is formed, which is expected to be catalytically relatively inactive towards hydroformylation, but enhances the isomerisation of the alk-1-enes to less-reactive internal alkenes. Here, we report our findings on phosphite-modified Co-catalysed hydroformylation using a ligand with a significantly larger *Tolman* cone angle [12]. The increased cone angle of tris(2,4-di-*tert*-butylphenyl)phosphite (175°) compared to $P(OPh)_3$ (128°) [12] is assumed to prevent the formation of the catalytically inactive bis(phosphito)cobalt hydride.

Experimental. *General.* All manipulations of air- and moisture-sensitive compounds were performed by means of standard *Schlenk* techniques under prepurified N_2 [13]. Toluene was distilled from Na, and THF from Na/benzophenone prior to use [14]. All other solvents were used as received. $[Co_2(CO)_8]$ was purchased from *Strem Chemicals* and stored at 4° under N_2 in a *Schlenk* tube wrapped with Al foil. The C_9-C_{11} paraffin cut (C_8 3, C_9 26, C_{10} 29, C_{11} 33, C_{12} 9%) and pent-1-ene (> 99%), a *Fischer–Tropsch* derived product, was supplied by *Sasol*. *Syngas* ($[CO]/[H_2] = 0.5$) was purchased from *Afrox*. All other reagents were purchased from *Sigma-Aldrich* and used as received. UV and IR Data: ν_{max} in cm^{-1} (rel. int. %). NMR Data: δ in ppm rel. to $SiMe_4$.

Synthesis of [$Co_2(CO)_6$[P(O-2,4-t-$Bu_2C_6H_3)_3$]$_2$] (**6**). The synthesis of compound **6** was similar to that of the related complex $[Co_2(CO)_6\{P(OPh)_3\}_2]$ [11][15]. Tris(2,4-di-*tert*-butylphenyl)phosphite (1.83 g, 2.83 mmol) was added to a soln. of $[Co_2(CO)_8]$ (0.422 g, 1.2 mmol) in toluene (10 ml). Gas evolution was observed immediately. The mixture was stirred and heated to 50°. IR Spectroscopy showed mainly dimer formation. The mixture was stirred overnight. The volatiles were removed *in vacuo*, and the solid was washed with pentane (2 × 10 ml). The straw-coloured solid was dried *in vacuo* to give **6**. Crystals suitable for X-ray diffraction (see below) were obtained from a sample acquired from an HP-IR run after one year. Yield: 1.76 g (93%). IR (CH_2Cl_2): 2002 (22), 1984 (100; ν(CO)). IR (KBr): 2963 (84, ν(CH)), 2871 (21, ν(CH)), 2005 (34, ν(CO)), 1987 (100, ν(CO)), 1979 (92, ν(CO)), 1494 (48, δ_{as}(Me)), 1400 (23), 1363 (31), 1262 (30), 1210 (32, ν(PO)), 1186 (49), 1161 (20), 1081 (70), 689 (31), 914 (35), 876 (46), 818 (30, Ar), 517 (29). ^{1}H-NMR (300 MHz, $CDCl_3$): 7.43, 7.03, 6.92 (arom. H); 1.24 (Me), 1.20 (Me). ^{13}C-NMR (75.5 MHz, $CDCl_3$): 148.19; 146.51; 138.51; 124.58; 123.57; 119.40; 34.94; 34.39; 31.32; 30.27. ^{31}P-NMR (121.5 MHz, $CDCl_3$): 156.36.

Synthesis of [$CoH(CO)_3$[P(O-2,4-t-$Bu_2C_6H_3)_3$]] (**2**). DMF (2.0 ml, 25.8 mmol) was added to a stirred soln. of $[Co_2(CO)_8]$ (1.699 g, 4.95 mmol) in toluene (10 ml). A pink precipitate ($[Co(DMF)_6][Co(CO)_4]_2$) formed within 1 h, and the supernatant completely decoloured. The mixture was cooled to 0°, and conc. HCl was added (6.0 ml). Immediately, a blue aq. phase and a light-yellow org. phase separated. The mixture was stirred for 30 min, after which the aq. phase was removed by syringe. The org. phase was washed with conc. HCl (3 × 1.0 ml). IR Spectroscopy showed the presence of $[CoH(CO)_4]$. Then, P(O-2,4-*t*-$Bu_2C_6H_3)_3$ (2.135 g, 3.3 mmol) was added and gas evolution was observed. IR Spectroscopy showed the presence of **2** (*ca.* 1 ml of the soln. was added to 1 g of ligand and allowed to react; IR analysis showed **2** as the only cobalt carbonyl species). The soln. was stored in a freezer, and a white solid crystallised. The mother liquor was removed, and the compound was dried *in vacuo*. IR (toluene): 2071 (CO, 47), 2020 (CO, 59), 1998 (100, toluene). ^{1}H-NMR (300 MHz, C_6D_6): 7.89 (*m*, 1 arom. H); 7.53 (*s*, 2 arom. H.); 1.71 (*s*, *t*-Bu); 1.16 (*s*, *t*-Bu); −11.04 (*d*, ^2J(P,H) = 13.5 Hz). ^{13}C-NMR (75.4 MHz, C_6D_6): 148.77; 147.08; 139.27; 125.08; 124.19; 120.14; 35.42; 34.50; 31.40; 30.72. ^{31}P-NMR (121.4 MHz, C_6D_6): 149.08.

IR Experiments. All IR spectra were recorded on a *Bruker Equinox-55* FT-IR spectrometer and analysed with the *Bruker* OPUS-NT software (32 scans, 4 cm^{-1} resolution, *Blackman–Harris* 3-term apodisation). Data for solns. of **2** and **6** were collected using NaCl windows (optical pathlength 0.1 mm). The high-pressure (HP) experiments were carried out in a 55-ml *SS-316* autoclave equipped with a mechanical stirrer (750 r.p.m.), temperature control, and pressure control (University of Amsterdam) [16]. The soln. was pumped through a bypass in which ZnS windows were embedded (optical pathlength at 25°: 0.3 mm).

The autoclave was flushed with Ar gas prior to use. A soln. of dimer **6** ([Co] = 1500 ppm (mg/kg solvent) in the final volume) in degassed solvent (10 ml) was transferred under Ar to the autoclave. The appropriate amount of ligand was added, and the assembled autoclave was purged with *Syngas* (3 ×). The autoclave was then pressurised at r.t. to 15 bar, resulting in a final pressure of *ca.* 20 bar at 140°. When the autoclave had reached the reaction temp., pentene (2 ml) was injected from an attached sample reservoir to give a total reaction pressure of 50 bar *Syngas*. Absorbance values at fixed wavelengths were fitted to the appropriate equations [17] using the SCIENTIST least-squares program [18]. After the reaction, GC samples were taken from the cooled, depressurised soln. ^{31}P-NMR Spectra of samples taken from the cooled and depressurised solution showed the presence of only **2**, **6**, and free phosphite ligand.

NMR Experiments. NMR Spectra were recorded on a *Varian Inova* spectrometer (^{1}H: 300 MHz, ^{13}C: 75.5 MHz, ^{31}P: 121.5 MHz) at ambient temp. The spectra were referenced rel. to $SiMe_4$ (^{1}H and ^{13}C) or 85% H_3PO_4 (^{31}P), using residual solvent signals (δ(H) 7.27 or 7.16 for $CHCl_3$ and C_6D_5H, resp.), the actual solvent resonances (δ(C) 77.0 and 128.0 for $CDCl_3$ and C_6D_6, resp.), or externally (^{31}P). HP-NMR experiments were performed in a 10-mm high-pressure ROE cell [19]. For these experiments, the required amount of dimer **6** was weighed in an Ar-filled sample tube, dissolved in C_6D_6 (1 ml), and transferred into the NMR tube *via* syringe. The appropriate amount of P(O-2,4-*t*-$Bu_2C_6H_3)_3$ was dissolved in C_6D_6 (1 ml), and transferred under Ar into the NMR tube. The cell was purged with *Syngas* (3 ×), pressurised to 40 bar, and left under pressure overnight (*ca.* 15 h) to allow proper gas dissolution.

Batch Autoclave Experiments. Gas-uptake experiments were performed with a stainless-steel batch autoclave (300 ml; *Parr* model *4560*). The autoclave – equipped with electrical heating, magnetic-drive gas-dispersion stirrer, and sample dip tube – was flushed with Ar prior to use. Required amounts of **6** and ligand (L) were dissolved in degassed paraffin (50 ml). The assembled autoclave was purged with *Syngas* (3×) before being pressurised to 20 bar. When the autoclave setup had reached the desired temp., pent-1-ene was injected from a 150-ml sample bomb, and the final reaction pressure was adjusted. The gas uptake of a thermostatted, 1-l gas reservoir was monitored by electronic pressure detection and used to calculate the reaction progress. End-of-run samples were analysed with an *Agilent 6890* GC system equipped with a *Hewlett-Packard Pona* column (50 m × 0.5 μm). Temp. program: 100° (hold 10 min), 250° (2°/min), 250° (5 min hold), 300° (10°/min), 300° (5 min). N_2 Carrier-gas flow was kept constant at 0.7 ml/min.

X-Ray Crystallography[3]). Crystals of **6** (see *Scheme 2*) were grown from paraffin as described above. X-Ray-diffraction data were collected on a *Siemens SMART CCD* diffractometer using MoK_α radiation (0.71073 Å) and ω-scans at 293(2) K. After collection, the first 50 frames were repeated to check for decay, which was not observed. All reflections were merged and integrated with SAINT [20], and were corrected for *Lorentz*, polarization, and absorption effects by means of SADABS [21]. The structures were solved by the heavy-atom method, and refined through full-matrix least-squares cycles using the SHELXL97 [22] software package, with $\Sigma(|F_o| - |F_c|)^2$ being minimised. All non-H-atoms were refined with anisotropic displacement parameters, while the H-atoms were constrained to parent sites by means of a riding model. The *t*-Bu groups in *para* position, all showing *ca.* 70% statistical disorder on the Me groups, were restrained by allowing limited anisotropic movement, using ISOR in SHELXL97. The DIAMOND (Visual Crystal Structure Information System) software [23] was used for the graphics. Crystal data and details of data collection and refinement are given in *Table 1*.

Results and Discussion. – *Synthesis.* The dinuclear complex $[Co_2(CO)_6\{P(O\text{-}2,4\text{-}t\text{-}Bu_2C_6H_3)_3\}_2]$ (**6**) was synthesised from dicobalt octacarbonyl and an excess of tris(di-2,4-*tert*-butylphenyl)phosphite as ligand (*Scheme 2*). We recently reported the molecular structure of the ligand [24], as well as its behaviour in the presence of Rh-based hydroformylation catalysts. The synthesis of dimer **6** is similar to that of the previously reported $P(OPh)_3$ complex $[Co_2(CO)_6\{P(OPh)_3\}_2]$ [15]. Complex **6** was obtained in excellent yields (90–95%) and characterised by IR, ^{1}H-, ^{13}C- and ^{31}P-NMR. Crystals of **6** suitable for X-ray diffraction could be obtained from the decomposition of hydride **2**. Compound **6** was used as starting material for the HP-IR, HP-NMR, and batch autoclave reactions.

The hydrido complex $[CoH(CO)_3\{P(O\text{-}2,4\text{-}t\text{-}Bu_2C_6H_3)_3\}]$ (**2**) was obtained by reacting $[CoH(CO)_4]$ (**1**) with 1 equiv. of the ligand (*Scheme 2*). The product was a light-yellow, crystalline solid, which was moderately O_2- but not moisture-sensitive. It was thermally sensitive at atmospheric pressure, and dimerised above 0° as a solid, and above −20° in solution.

Reaction of **2** with excess phosphite (up to 100 equiv.) did not result in formation of the bisphosphito complex $[CoH(CO)_2\{P(O\text{-}2,4\text{-}t\text{-}Bu_2C_6H_3)_3\}_2]$, as confirmed by IR spectroscopy (ν(CO) in toluene). This is in contrast to the formation of the bisphosphito hydride when using phosphites with smaller *Tolman* cone angles [12] such as $P(OPh)_3$ [11].

Solid-State Structure of Compound **6**. A molecular diagram showing the numbering scheme and thermal ellipsoids for **6** is given in *Fig. 1*; selected geometric parameters are

---

[3]) The crystallographic data for **6** have been deposited with the *Cambridge Crystallographic Data Centre* (*CCDC*) as supplementary publication number CCDC-266164. Copies of the data can be obtained, free of charge, by application to CCDC, 12 Union Road, Cambridge, CB2 1EZ, UK (fax: +44-1223-336033; e-mail: deposit@ccdc.cam.ac.uk), or *via* the internet (http://www.ccdc.cam.ac.uk/products/csd/request).

Table 1. *Crystal Data and Structure Refinement for* **6**

Empirical formula	$C_{93}H_{150}Co_2O_{12}P_2$
Formula weight	1639.93
Temperature [K]	293(2)
Crystal size	$0.30 \times 0.26 \times 0.04$ mm
Wavelength [Å]	0.71069
Crystal system, space group	Triclinic, $P\bar{1}$
a [Å]	11.833(5)
b [Å]	13.147(5)
c [Å]	18.249(5)
α [°]	100.205(5)
β [°]	97.546(5)
γ [°]	114.740(5)
Volume [Å^3]	2469.7(16)
Z, calc. density [Mg m^{-3}]	1, 1.103
Absorption coefficient [mm^{-1}]	0.421
$F(000)$	888
θ Range [°]	5.10 to 25.35
Index ranges	$-14 \le h \le 14,\ -12 \le k \le 15,\ -21 \le l \le 21$
Reflections collected/unique/R_{int}	13398/8880/0.0746
Completeness to 2θ	98.1%
Max. and min. transmission	0.9838, 0.8872
Refinement method	Full-matrix least-squares on F^2
Data/restraints/parameters	8880/138/616
Goodness-of-fit on F^2	0.984
Final R indices [$I > 2\sigma(I)$]	$R1 = 0.0690$
	$wR2 = 0.1523$
R Indices (all data)	$R1 = 0.1580$
	$wR2 = 0.1912$
Largest diff. peak and hole [e Å^{-3}]	0.531 and -0.333

Scheme 2. *Synthesis of Dimer* **6** *and Hydride* **2**

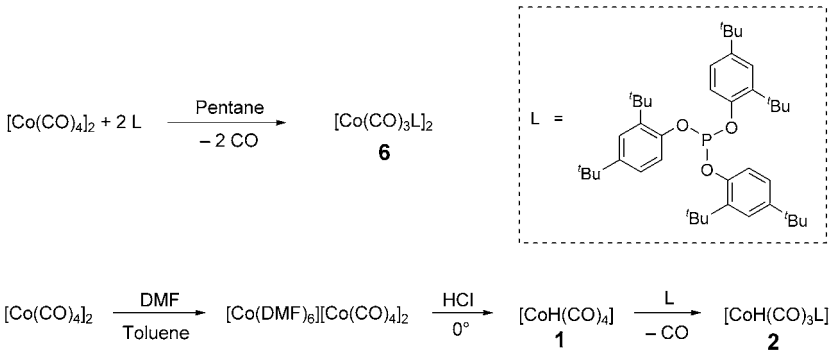

summarised in *Table 2*. *Fig. 1* clearly shows a dinuclear arrangement formed by two trigonal [$Co(CO)_3L$] fragments, two phosphite ligands being in *trans* positions with respect to the Co–Co bond (2.706(5) Å). The molecule has an inversion centre, which bisects the Co–Co bond, and the phosphite ligands have a measured cone angle of 176°. A trigonal plane is defined by the three CO ligands, and the Co-atom is displaced by 0.193(3) Å towards the apical phosphite ligand.

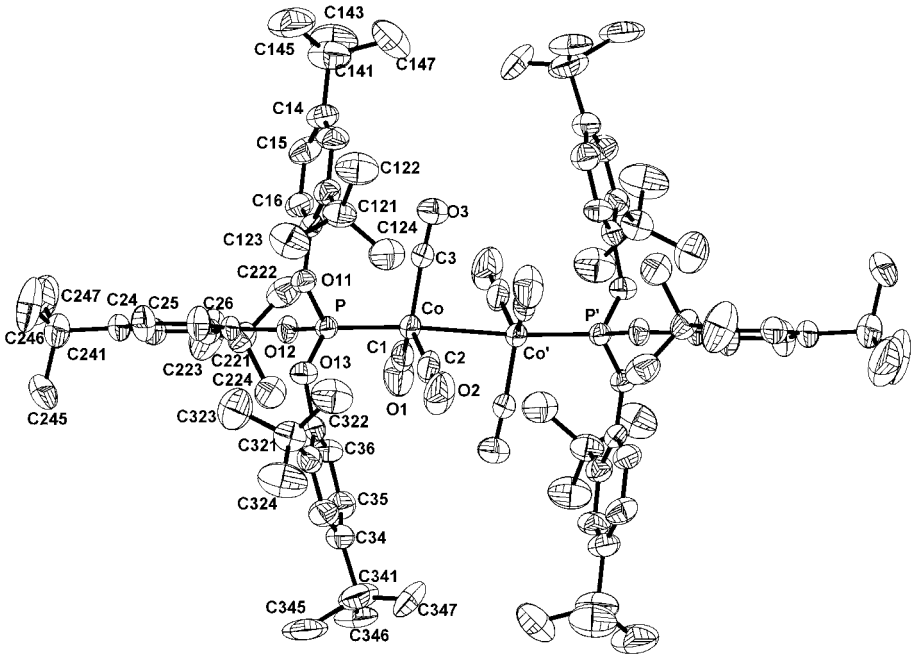

Fig. 1. *X-Ray crystal structure of* $[Co_2(CO)_6\{P(O\text{-}2,4\text{-}t\text{-}Bu_2C_6H_3)_3\}_2]$ (**6**) (50% probability). The H-atoms and the statistical disorder (*ca.* 70%) at the *p-t*-Bu groups are omitted for clarity. For the Ph rings, the first digit refers to the ring number, while the second digit indicates the number of the C-atom in the ring. Primed atoms were generated *via* the crystallographic inversion centre.

Table 3 compares the geometric parameters of **6** with those of known, similar complexes. The distortion induced in these types of compounds is evident, more-bulky ligands showing more-significant effects. The distortion due to the (sterically demanding) phosphorus donor ligands is manifested in the displacement of the Co-atom from the trigonal plane formed by the three CO ligands, as well as by the lengthening of the Co–Co bond. This is assumed to be due to the steric demand of the $P(O\text{-}2,4\text{-}t\text{-}Bu_2C_6H_3)_3$ ligands, which introduce intramolecular crowding at the CO ligands, causing a larger distortion, as manifested by the out-of-plane distance (0.193(3) Å; trigonal plane formed by the three CO C-atoms) of the individual Co-atoms. This distortion is further observed in the P–Co–CO angles. We are currently further investigating the influence of phosphorus donor ligands on the displacement of Co-atoms in associated complexes.

High-Pressure IR Experiments. The formation of the active hydroformylation species, $[CoH(CO)_3\{P(O\text{-}2,4\text{-}t\text{-}Bu_2C_6H_3)_3\}]$ (**2**), was studied at various ligand/Co ratios by heating a mixture of $P(O\text{-}2,4\text{-}t\text{-}Bu_2C_6H_3)_3$ and dimer $[Co_2(CO)_6\{P(O\text{-}2,4\text{-}t\text{-}Bu_2C_6H_3)_3\}_2]$ (**6**) under *Syngas* pressures in paraffin. The Co concentration was varied between 1000 and 2400 ppm, with the [phosphite]/[Co] ratio varying between 4 : 1 and 20 : 1. The formation of the hydrido species was studied at temperatures and pressures of up to 180° and 80 bar. *Table 4* summarises these experiments and observations.

Table 2. *Selected Interatomic Bond Distances* (Å) *and Angles* (°) *of* **6**. Symmetry-related atoms are indicated.

Co–C(2)	1.767(9)	C(2)–Co–C(1)	120.53(32)
Co–C(1)	1.769(8)	C(2)–Co–C(3)	118.81(30)
Co–C(3)	1.792(9)	C(1)–Co–C(3)	117.14(33)
Co–P	2.134(4)	C(2)–Co–P	92.72(18)
Co–Co[a])	2.706(5)	C(1)–Co–P	96.69(18)
P–O(12)	1.589(6)	C(3)–Co–P	99.48(17)
P–O(13)	1.592(8)	C(2)–Co–Co[a])	83.33(18)
		C(1)–Co–Co[a])	82.70(18)
		C(3)–Co–Co[a])	85.21(17)
		P–Co–Co[a])	174.95(4)
		O(2)1–P–O(13)	104.18(20)
P–O(11)	1.596(5)	O(12)–P–O(11)	106.14(21)
O(1)–C(1)	1.146(8)	O(13)–P–O(11)	91.60(19)
O(2)–C(2)	1.137(9)	O(12)–P–Co	113.06(12)
O(3)–C(3)	1.124(10)	O(13)–P–Co	120.00(12)
O(11)–C(11)	1.399(8)	O(11)–P–Co	118.98(13)
O(12)–C(21)	1.410(6)	O(1)–C(1)–Co	178.65(66)
O(13)–C(31)	1.399(8)	O(2)–C(2)–Co	178.55(65)
		O(3)–C(3)–Co	176.16(58)
		C(11)–O(11)–P	124.46(36)
		C(21)–O(12)–P	131.86(28)
		C(31)–O(13)–P	126.50(31)

[a]) $-x, 1-y, -z$.

Table 3. *Structural Correlations for Complexes of the Type* $[Co_2(CO)_6\{L\}_2]$ (L = PX_3, X = alkyl, alkoxy, or aroyl)

	Distance [Å]				Angle [°]		Ref.
Ligand (L)	Co–Co	Co–P	Co–(CO)[a])	d[b])	P–Co–CO	P–Co–Co	
CO	2.522(1)	–	1.82(1) 1.93(1)[d])	[c])	–	–	
$P(OPh)_3$	2.6722(4)	2.1224(4)	1.783(2)	0.158(1)	95.0	177.3(2)	[11]
$P(O\text{-}2,4\text{-}^tBu_2C_6H_4)_3$	2.706(5)	2.134(4)	1.776(7)	0.193(3)	96.3(2)	174.95(4)	[e])
$P(O^iPr)_3$	2.6544(12)	2.1350(12)	1.769(2)	0.070	92.3	177.00(6)	[25]
$P(^nBu)_3$	2.665(14)	2.178(15)	1.75(3)	–	–	180	[26]
PMe_3	2.669(1)	2.175(1)	1.772(3)	0.104	93.4	180	[27]

[a]) Average of equivalent values. [b]) Distance of Co from trigonal plane as calculated from data obtained from CSD. [c]) Square pyramidal geometry due to bridging CO ligands. [d]) Bridging CO. [e]) This work.

The monosubstituted hydride **2** – having strong IR absorbances at 2071, 2021, and 2000 cm^{-1} – started to form at 105°, independent of Co concentration or ligand excess. At this temperature, the strong ν(CO) absorbance at 1984 cm^{-1}, typical for **6**, started to decrease in intensity, while the second characteristic absorption for the dimer (2000 cm^{-1}) was obscured by the hydride absorption. At 125°, these two bands (1984 and 2000 cm^{-1}) had disappeared completely in all experiments, regardless of Co concentration and ligand excess. Similar behaviour was also observed in HP-NMR studies in (D_6)benzene, where only the modified hydride **2** was observed at temperatures of up to 130° (pressure: *ca.* 50 bar) by ^{1}H- and ^{31}P-NMR.

Table 4. *Results of High-Pressure IR Studies on the Formation of* **2** *in Paraffin*

[Co]		[L]/[Co]	T_{MH}[b])	T_{Dimer}[c])	T_{UH}[d])	Pressure
[ppm]	[mM][a])		[°]	[°]	[°]	[bar]
1000	12.0	8:1	105	125	n.d.[e])	20–30
1400	17.2	4:1	105	125	135 (25)[f])	20–50
1400	17.2	8:1	105	125	n.d.	20–50
1800	22.1	8:1	105	125	140 (80)[f])	20–80
1800	22.1	20:1	100	120	n.d.	20–80
2400	28.8	8:1	105	125	n.d.	20–26

[a]) Concentration in starting solution at 1 bar and 25°. [b]) Temperature where **2** appeared. [c]) Temperature where **6** disappeared completely. [d]) Temperature where **1** appeared. [e]) Not detected. [f]) Pressure where **1** was formed.

Fig. 2 illustrates the formation of **2** and the disappearance of **6** monitored by IR in the temperature range between 55 and 140° at *Syngas* pressures of 20–26 bar. The Co concentration was 2400 ppm, with a [P(O-2,4-*t*-$Bu_2C_6H_3)_3$]/[Co] ratio of 8:1.

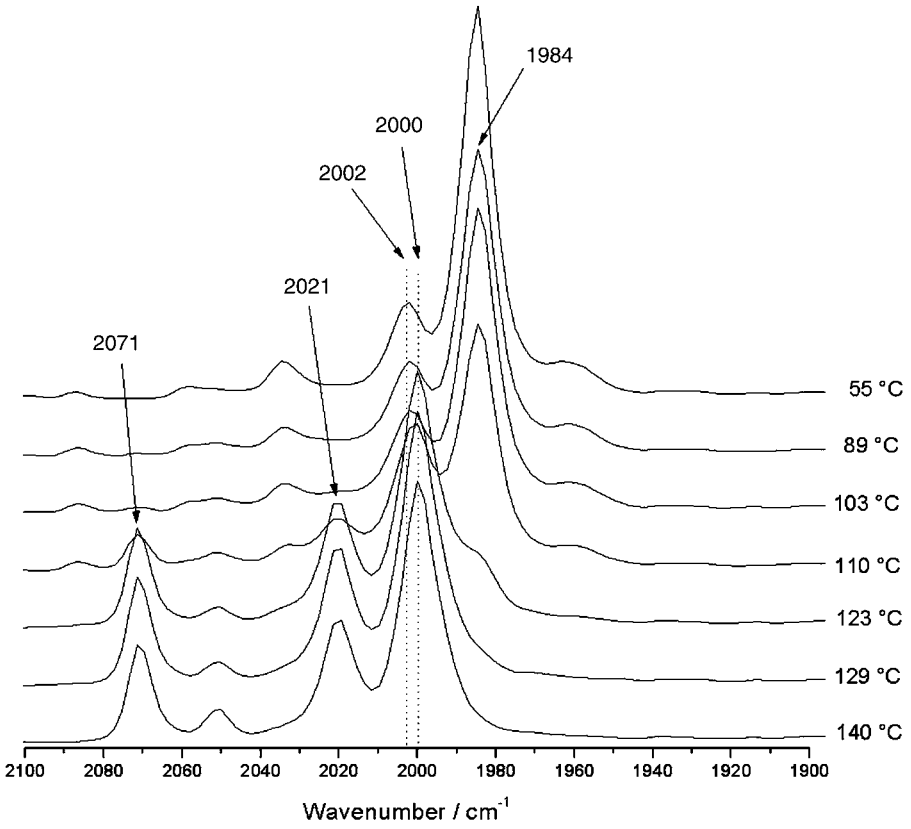

Fig. 2. *Temperature-dependent IR spectra showing the formation of modified hydride* **2** *from dimer* **6**. [Co] = 2400 ppm, [P(O-2,4-*t*-$Bu_2C_6H_3)_3$]/[Co] 8:1, starting pressure = 20 bar *Syngas*, solvent = paraffin.

No unmodified hydride, *i.e.*, $[CoH(CO)_4]$ (**1**), could be detected under the above conditions, even after deconvolution of the spectra. Complex **1** exhibits strong absorbance at 2030 cm^{-1}, which, since being close to the band of **2** at 2021 cm^{-1}, can appear as either a shoulder or a peak at high concentrations. The peak at 2053 cm^{-1}, however, suggests that small amounts of unmodified **1** do, in fact, form under these conditions.

The formation of complex **2** was studied in detail. Over a period of 40 min, a solution of **2** was kept at 105° and at 21 bar pressure. *Fig. 3* depicts the decrease of the dimer absorption at 1984 cm^{-1}, and the simultaneous increase of the absorption at 2000 cm^{-1} (for hydride **2**). It can be clearly seen that hydride formation at a certain temperature is time dependent, due to either a nonequilibrated solution or undissolved dimer particles.

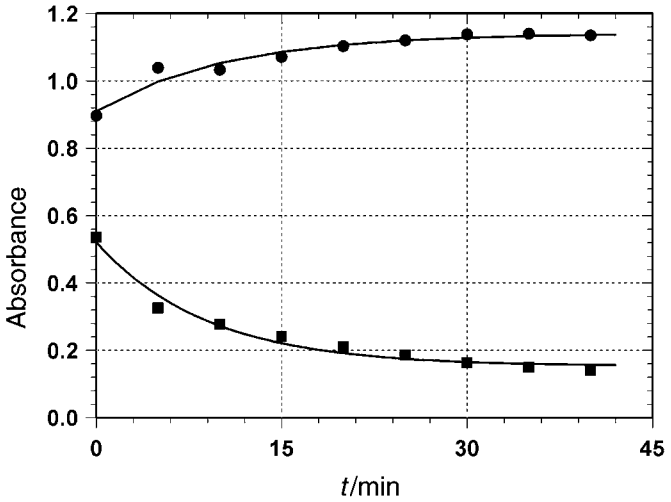

Fig. 3. *First-order kinetics for the formation of* **2**. Lower curve: decrease in the absorbance of ν(CO) at 1984 cm^{-1} of **6**; upper curve: increase in the absorbance of ν(CO) at 2071 cm^{-1} of **2**. Conditions: 105°, [Co] = 1800 ppm, $[P(O\text{-}2,4\text{-}t\text{-}Bu_2C_6H_3)_3]/[Co] = 8:1$, 21 bar *Syngas*, solvent = paraffin.

However, when we calculated the rate constants for hydride formation and dimer decrease, the values were, within experimental error, the same: $k_{Dimer} = 0.0019 \pm 0.0003$ s^{-1}, $k_{Hydride} = 0.0016 \pm 0.0003$ s^{-1}. This suggests that the way the dimer is split by dissolved H_2 occurs without the formation of intermediates.

The formation of the modified hydride **2** from the unmodified hydride **1** was studied in order to exclude the presence of **1** as far as possible under conditions with a ligand-to-metal ratio higher than 4 : 1. For these experiments, $[Co_2(CO)_8]$ at a concentration of 1500 ppm was dissolved in paraffin, and the formation of $[CoH(CO)_4]$ (**1**) was observed at 140° and 40 bar *Syngas* pressure. From the (weak) absorption at 1868 cm^{-1}, indicating bridging CO groups, we concluded that there is an equilibrium between $[Co_2(CO)_8]$ and $[CoH(CO)_4]$ (**1**) under these conditions (*Scheme 3*). The expected IR absorptions for **1** at 2115, 2053, 2030, and 1998 cm^{-1} were clearly observed.

Scheme 3. *Equilibria between [$Co_2(CO)_8$] and Hydrides* **1** *and* **2**. Conditions: [Co] = 1500 ppm, pressure = 40 bar *Syngas*, solvent = paraffin; L = P(O-2,4-*t*-$Bu_2C_6H_3)_3$.

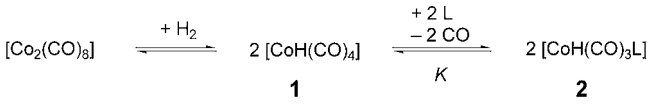

Fig. 4 further shows the HP-IR spectrum of **1** as a function of ligand concentration. Upon addition of ligand (> 0.5 equiv.) to a solution of **1**, the absorption at 1868 cm^{-1} disappeared. The absorptions due to **1** decreased, with a clear increase of the absorptions indicative of modified hydride **2**. After addition of 2.5 equiv. of ligand, the absorptions due to hydride **1** disappeared almost completely. Only a shoulder remained for the strongest absorption at 2030 cm^{-1}, which could be observed only after *Fourier* self-deconvolution. A small amount of unmodified **1** was also indicated by the absorbance at 2053 cm^{-1}. Based on this titration experiment (*Fig. 4*, *b*), an equilibrium constant *K* was calculated using an equation similar to that reported previously [17]. Thereby, the ν(CO) absorbance of **1** at 2053 cm^{-1} was taken, assuming that the CO pressure was constant, and taking into account that in the first spectrum approximately 30% of the dimer was still present. *K* was found to be 620 ± 60[4]) at 140° and 40 bar pressure. This confirmed that *ca.* 1–2% of unmodified **1** would be present under similar conditions (*i.e.*, [L]/[Co] = 8:1; [Co] = 1000 ppm; pressure = 40 bar; T = 140°).

To further ensure the absence of [$CoH(CO)_4$] (**1**) under the reaction conditions, pressure-variation experiments were performed at 150°. In *Fig. 5*, the IR spectra of **1**, recorded between 50 and 80 bar *Syngas* pressure, are shown. No absorbance at 2029 cm^{-1} could be detected, however, above 70 bar, the band at 2021 cm^{-1} broadened. After cooling the solution to room temperature under 20 bar of *Syngas*, the three ν(CO) absorptions for **2** were still observed. The ratio between the intensities of these three bands remained almost constant throughout the experiments. At 150° and 80 bar, the relative intensities (%) of the ν(CO) absorptions at 2000, 2021, and 2071 cm^{-1} were 100:56:39, while, at room temperature, they were 100:62:43, respectively. The relative IR intensities of separately synthesised **2** (in toluene) were 100, 59, and 47% at 1998, 2020, and 2071 cm^{-1}, respectively. From these excellent correlations, we concluded that the species observed at room temperature and 20 bar pressure is the same as the one observed at 150° and 80 bar. Furthermore, these results convinced us that the species observed in the high-pressure studies was indeed, the modified hydride **2**.

The stability of [$CoH(CO)_3${P(O-2,4-*t*-$Bu_2C_6H_3)_3$}] (**2**), was accounted for in various experiments. *Table 5* compiles the results of 50-min stability runs. Slight hydride decomposition was observed at a [L]/[Co] ratio of 8:1 at a temperature of 140° (*Entries 1–3*). Increasing the [L]/[Co] ratio to 12 resulted in a virtually stable system (*Entry 4*), even under more-drastic reaction conditions. Thus, if the resting state of the catalytic cycle (in this case [$CoH(CO)_3${P(O-2,4-*t*-$Bu_2C_6H_3)_3$}]) is stabilised by

---

[4]) When [CO] is constant and L corresponds to P(O-2,4-*t*-$Bu_2C_6H_3$), the following equation applies at equilibrium: $K = \frac{K'}{[CO]} = \frac{[\mathbf{2}]}{[\mathbf{1}][L]}$; see *Fig. 4*.

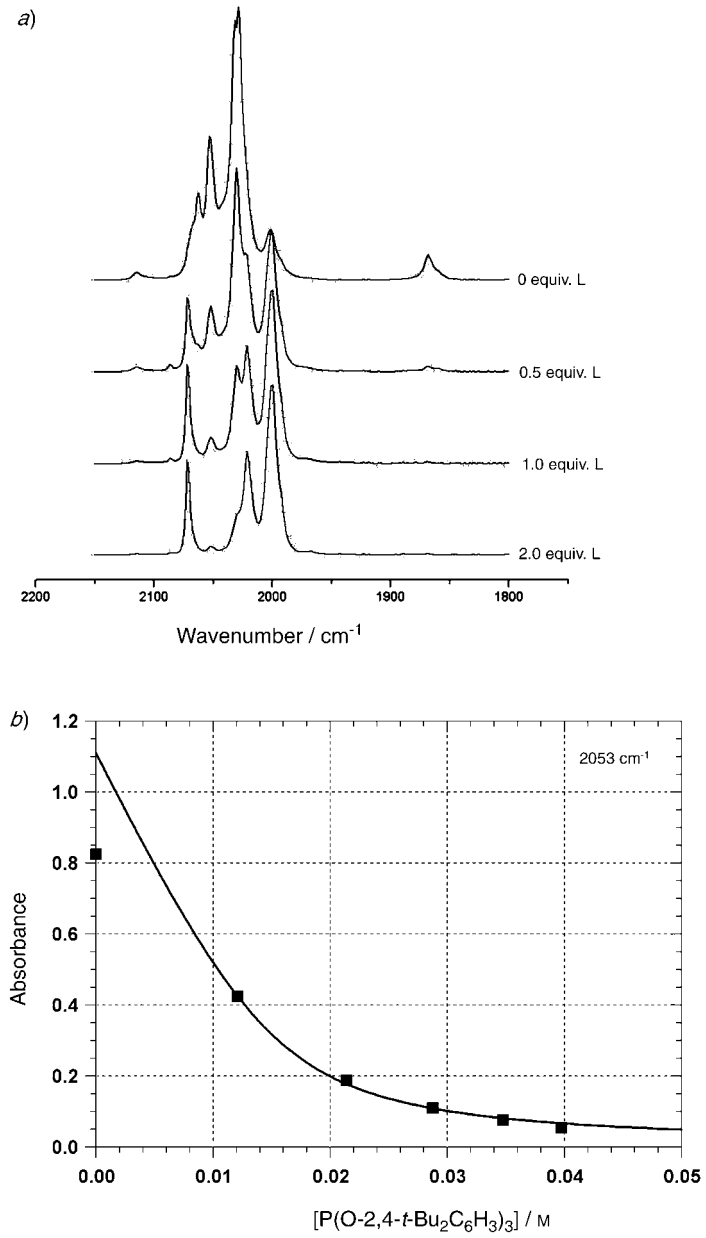

Fig. 4. a) *HP-IR Spectra of the equilibria between [$Co_2(CO)_8$], hydride* **1**, *and hydride* **2** *at 140° and 40 bar* Syngas *pressure in paraffin*. [Co] = 1500 ppm in final volume; L = P(O-2,4-*t*-$Bu_2C_6H_3)_3$. b) *Decrease in the IR absorbance at 2053 cm^{-1}, fitted to appropriate function*[2]).

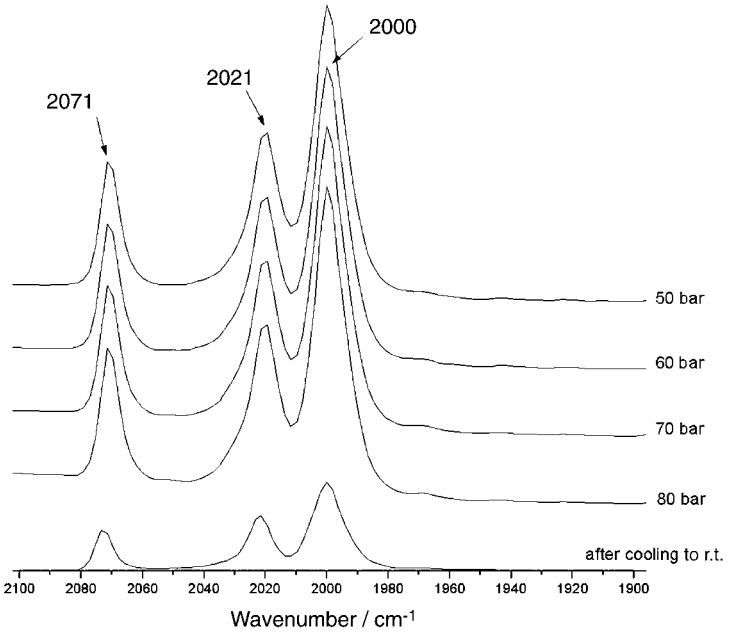

Fig. 5. *Stability of Complex* **6** *in paraffin at 150° between 50 and 80 bar* Syngas *pressure, as monitored by HP-IR.* [Co] = 1800 ppm, [P(O-2,4-*t*-$Bu_2C_6H_3)_3$]/[Co] 8:1, starting pressure = 20 bar.

Table 5. *Stability of Complex* **2** *in Paraffin, as Monitored by the Relative Change in Selected IR Absorptions.* L = P(O-2,4-*t*-$Bu_2C_6H_3)_3$.

Entry	[Co] [ppm]	[L]/[Co]	*T* [°]	Pressure [bar]	Rel. change [%][a])		
					2000	2021	2071
1	1800[b])	8:1	120	20	−2.3	−2.2	−0.8
2	1800	8:1	140	20	−8.0	−7.8	−6.9
3	1800[b])	8:1	140	50	−6.3	−4.8	−1.7
4	1800[b])	12:1	160	80	+0.4	−0.1	−0.5
5	2400	8:1	140	30	−3.6	−7.0	−5.7

[a]) IR Signals at 2000, 2021, and 2071 cm^{-1}, resp. [b]) Addition of pent-1-ene (hydroformylation reaction conditions).

excess ligand, the overall activity of the catalyst decreases. This was, indeed, observed in batch autoclave experiments (see below).

It was known from previous experiments with less-bulky ligands [11] that the formation of bis(phosphito)cobalt hydride species occurs at higher ligand-to-metal ratios. These hydride complexes proved to be less-active hydroformylation catalysts [11] than the monophosphite complexes. All experiments with P(O-2,4-*t*-$Bu_2C_6H_3)_3$ as ligand were conducted with a minimum [phosphite]/[Co] ratio of 4:1. No bis(phosphito)cobalt hydride was observed under these conditions at 1000, 1400, and 1800 ppm

Co concentration, and increasing this ratio up to 20:1 ([L] *ca.* 0.44M at 1 bar, 25°) did not lead to the formation of a bis(phosphito)cobalt hydride species either. This observation is in agreement with the synthetic study, where the bis(phosphito)cobalt hydride could not be obtained. The latter should display a different absorbance pattern, with three ν(CO) bands at *ca.* 2034, 2000, and 1973 cm^{-1}, as was observed for $P(OPh)_3$ [11]. Since no such species was observed with $P(O\text{-}2,4\text{-}t\text{-}Bu_2C_6H_3)_3$, the concept of using very large cone angles to prevent higher substitution on the Co centre proved to be valid.

To obtain more information on the catalytic activity of modified hydride **2**, we performed a number of hydroformylation runs at *Syngas* ([CO]/[H_2] 1:2) pressures between 40 and 60 bar, and temperatures between 140 and 170°. The reactions were run in paraffin (octane) as a solvent. In these experiments, a Co concentration of 1000 ppm was used to enable correlation with the batch autoclave experiments. After preforming **2** at the desired temperature (starting pressure of *ca.* 30 bar), pent-1-ene was added, and the pressure was increased to the predetermined final pressure, which was maintained for the duration of the hydroformylation experiment.

Repeated scans indicated that hydride **2** was, indeed, an active hydroformylation catalyst. An increase of the IR absorption at 1734 cm^{-1}, indicative of aldehyde formation, was observed, together with a decrease in the absorptions at 1640 and 1825 cm^{-1}, indicative of alk-1-ene, respectively (*Fig. 6,a*). During the hydroformylation reaction, the IR spectrum of **2** did not change. No other absorptions in the CO region (other than aldehyde absorption) were observed, indicating that **2**, indeed, corresponds to the resting state of the catalyst. *Fig. 6,a* shows an overlay of selected IR spectra of a typical run (spectra recorded at 1, 2, 3, 5, 7, 10, 15, 20, 25, 30, and 40 min, resp.). *Fig. 6,b* shows the increase of the absorption at 1734 cm^{-1}, and the decrease of those at 1640 and 1825 cm^{-1} with time.

Assuming the absorption in the mixture to be linear with concentration, the observed rate constant k_{obs} for pent-1-ene conversion was calculated according to the first-order rate law (*Eqn. 1*):

$$-\frac{\delta[\text{pentene}]}{\delta t} = k_{obs}[\text{pentene}] = k_{obs}[\text{aldehyde}] \quad (1)$$

The results of these HP-IR hydroformylation experiments are compiled in *Table 6*. The absorption at 1825 cm^{-1} is unique for alk-1-enes and, thus, well-suited to calculate k_{obs} for the consumption of pent-1-ene. The olefin can be hydroformylated to the desired aldehyde, isomerised to internal pentenes, and hydrogenated to pentane. GC Analysis of end-of-run samples showed no paraffin formation. Therefore, hydrogenation to pentane could, under these conditions, be discounted. The k_{obs} value obtained for the absorption at 1734 cm^{-1} accounts for aldehyde synthesised in the system, which is a combination of both linear and branched aldehydes. The k_{obs} values correlated to the resonances at 1640, 1825, and 1734 cm^{-1} were all similar within experimental error; only the values for 1734 cm^{-1} are, thus, given in *Table 6*.

The systems studied by HP-IR and by batch autoclave runs were significantly different (stirring, reactor design, olefin concentration, *etc.*). Nevertheless, the calculated k_{obs} values turned out to be comparable, and a similar trend in the values

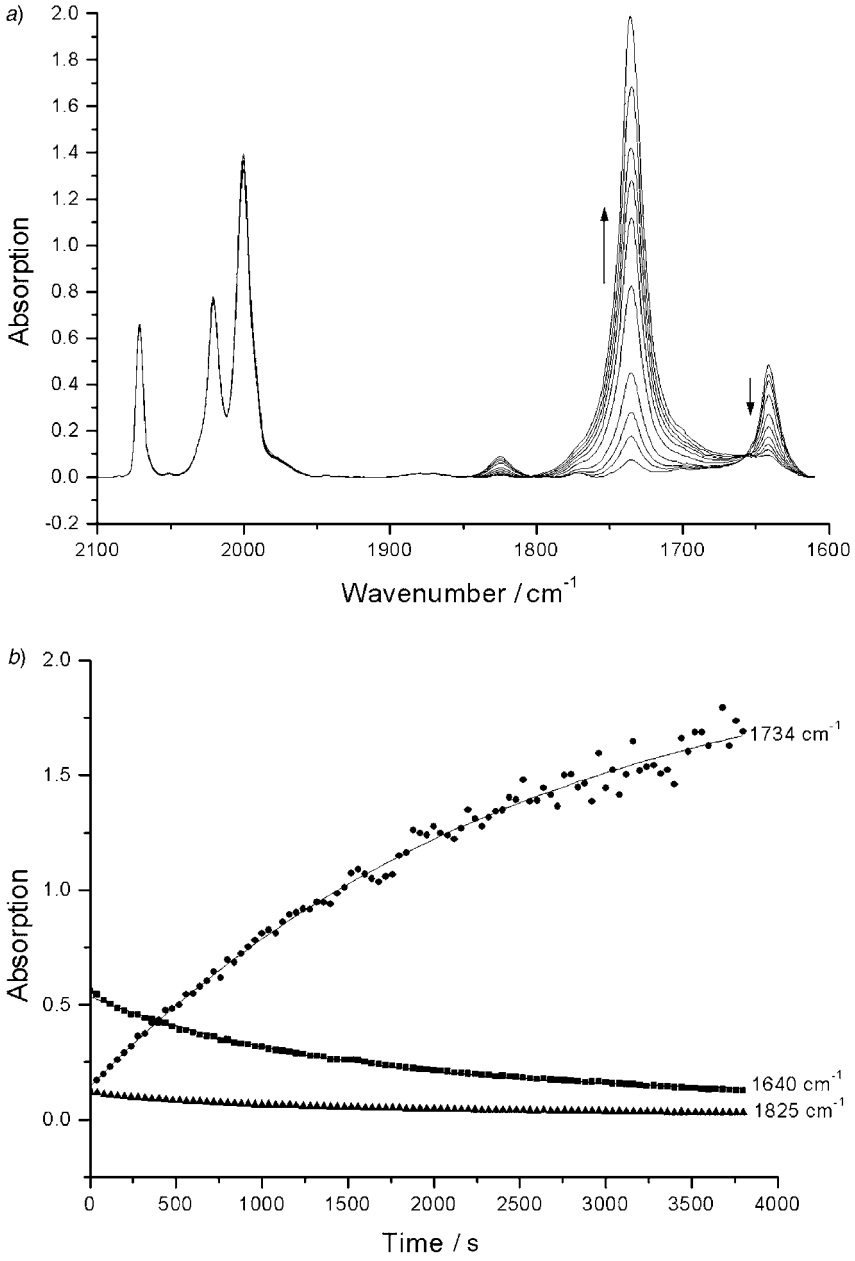

Fig. 6. a) *Overlayed HP-IR spectra of the hydroformylation of pent-1-ene at 140° in paraffin*. [Co] = 1000 ppm, [P(O-2,4-*t*-$Bu_2C_6H_3)_3$]/[Co] 8 : 1, pressure = 50 bar *Syngas*. b) *Increase and decrease of the absorptions at 1734, 1640, and 1825 cm^{-1} for the above run*.

Table 6. *Rate of Pent-1-ene Hydroformylation in the Presence of Complex* **2** (as determined from the change in IR absorption at 1734 cm^{-1}). [Co] = 1000 ppm, solvent = paraffin, L = P(O-2,4-*t*-$Bu_2C_6H_3)_3$.

Entry	T [°]	Pressure [bar]	[L]/[Co]	k_{1734} [10^3 s^{-1}]
1	140	50	0:1	14 ± 2
2	140	50	8:1	0.73 ± 4
3	140	50	19:1	0.09 ± 1
4	150	50	8:1	0.36 ± 3
5	150[a])	50	8:1	1.76 ± 2
6	160	50	8:1	1.14 ± 9

[a]) [Co] = 1500 ppm.

was observed. At high phosphite concentrations (*Entry 3*, *Table 6*) a decrease in k_{obs} was observed. The exact reason is not clear yet, but will be addressed in subsequent investigations.

Batch Autoclave Experiments. Batch autoclave experiments were carried out using paraffin as a solvent. A Co concentration of 1000 ppm was used for gas-uptake measurements. The kinetics were studied at 50 bar *Syngas* ([CO]/[H_2] 1:2 pressure) between 120 and 170°. The gas uptake of a 1-l vessel was used to calculate the reaction progress. The gas uptake as a function of time was used to estimate rate constants; in some experiments, samples were taken at timed intervals over a period of 4 h. GC Analysis of the samples resulted in time-dependent conversion curves, as depicted in *Fig. 7*. From these curves, the observed rate constant for pent-1-ene conversion was obtained according to *Eqn. 1*. The results of these batch autoclave hydroformylation experiments are compiled in *Table 7*.

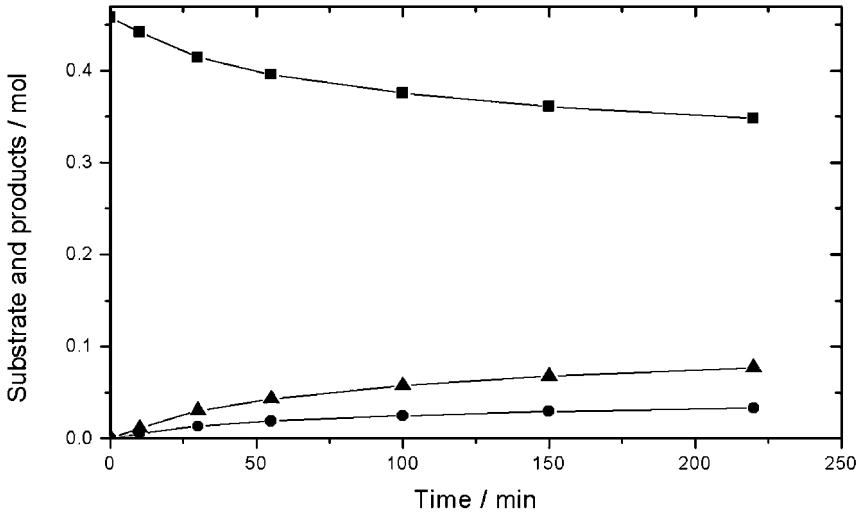

Fig. 7. *Sampling results for the hydroformylation of pent-1-ene at 140°* (*Entry 5* in *Table 7*). [Co] = 980 ppm, [P(O-2,4-*t*-$Bu_2C_6H_3)_3$]/[Co] 8:1, pressure = 60 bar *Syngas*. Symbols: ■ = pent-1-ene, ▲ = unbranched aldehyde, ● = branched aldehyde.

Kinetic data for 'unmodified' and '$P(OPh)_3$-modified' hydroformylation of pent-1-ene are given in *Entries 1* and *2*, respectively, of *Table 7* [11]. In general, the rate for phosphite-modified Co-catalysed transformation is very low compared to that with the unmodified one. None of the experiments in the present study have been optimised, and, therefore, comparison of different catalysts should only be made under identical conditions. With the new catalyst, aldehydes were the main product, and only a small amount of hydrogenation products were observed. In contrast, hydroformylation of pent-1-ene using $P(OPh)_3$ as a ligand resulted mainly in the formation of internal alkenes due to isomerisation of pent-1-ene [11]. We proposed that this isomerisation is catalysed by the bis(phosphito)cobalt hydride species. In the current system, we have observed neither internal alkenes nor the bis(phosphito)cobalt hydride species by means of HP-IR studies.

Based on *Entries 3–7* (*Table 7*), an activation energy of 71.8 kJ/mol was calculated from an *Arrhenius* plot. This value agrees with literature data of 77 kJ/mol [28] and 95 kJ/mol [29] for hydroformylation with modified homogeneous Co catalysts. The k_{obs} values determined by gas-uptake measurements were in good agreement with those calculated from sampling runs (*Entries 4* and *5*). When decreasing the metal concentration by 47% from 980 to 520 ppm (*Entry 5 vs. 8*), the rate constant droped by 41% to 0.17×10^{-3} s^{-1}, indicating an almost linear relationship between reaction rate and catalyst concentration.

Table 7. *Kinetics of Hydroformylation of Pent-1-ene in the Presence of Catalyst* **2** *in Paraffin*. Batch autoclave experiments at [Co] = 1000 ppm, L = P(O-2,4-*t*-$Bu_2C_6H_3)_3$ (see *Exper.*).

Entry	T [°]	Pressure [bar]	[L]/[Co]	k_{obs}[a]) [10^3 s^{-1}]
1[b])	140	50	0 : 1	3.22×10^3
2[b])	140	50	8 : 1	0.13
3	120	50	8 : 1	0.20
4	140	50	8 : 1	0.29
5	140[c])	60	8 : 1	0.29
6	150	50	8 : 1	1.38
7	170	50	8 : 1	1.90
8	140[d])	60	8 : 1	0.17
9	170	50	18 : 1	1.26

[a]) Standard deviations *ca.* 15%. [b]) $P(OPh)_3$ as ligand, from [11]. [c]) 980-ppm Co sampling run using sample dip tube (*Fig. 7*). [d]) [Co] = 520 ppm.

The ligand concentration seems to have a retarding effect on the rate constant (*Entries 7* and *9* in *Table 7*), as was already observed in the HP-IR studies. This behaviour is known among metal (*e.g.*, Rh) complexes that can coordinate more than one ligand; and we recently demonstrated the deactivation of Co catalysts by triphenylphosphite [11]. Here, the situation seems to be different, since no hydrides containing more than one phosphite ligand were observed in either the synthesis or HP-IR studies. From the equilibrium constant, however, it can be calculated that small amounts of unmodified hydride might be present under these conditions. The unmodified hydride **1** has a rate constant at least 20 times higher than the modified hydride **2** (see HP-IR hydroformylation experiments). This means that only 2% of **1**

([Co] = 1500 ppm; [L]/[Co] 8:1) would lead to an overestimation of k_{obs} by *ca.* 0.2×10^{-3} s^{-1} (based on *Entry 1* in *Table 6*).

From the sampling runs using a [L]/[Co] ratio of 8:1, the l/b (linear *vs.* branched aldehyde) ratio was determined to be 2.9 (74% unbranched) in case of 980 ppm Co, and 2.3 (70% unbranched) in case of 540 ppm Co, respectively. This product distribution is less favourable (less unbranched aldehyde) than the ones determined for the smaller $P(OPh)_3$ ligand studied previously. However, our bulky phosphite ligand resulted in a ten times more-active catalyst system.

Conclusions. – The complex $[Co_2(CO)_6\{P(O\text{-}2,4\text{-}t\text{-}Bu_2C_6H_3)_3\}_2]$ (**6**) was synthesised in good yield and characterised by IR and NMR spectroscopy and by crystallography. The proposed hydride intermediate $[CoH(CO)_3\{P(O\text{-}2,4\text{-}t\text{-}Bu_2C_6H_3)_3\}]$ (**2**) was synthesised and characterised by IR and NMR spectroscopy, but, due to its low thermal stability, no elemental analysis or mass spectrometric data could be obtained.

The dimer **6** was used as a precursor in the hydroformylation of pent-1-ene. High-pressure (HP) IR studies revealed that, under typical reaction conditions, only hydride **2** was present. The absence of the corresponding bis(phosphito)cobalt hydride was rationalised by the large cone angle of the phosphite moiety. HP-IR studies revealed that the unmodified hydride $[CoH(CO)_4]$ (**1**) was present in very low concentrations at [phosphite]/[Co] ratios higher than 4:1. Batch autoclave experiments indicated only modified hydrides, since the activity of **1** is three orders of magnitude higher than that of **2**. The reaction rate was dependent on both the catalyst and the ligand concentration, and the activation energy for the hydroformylation of pent-1-ene was calculated to be 71.8 kJ/mol.

Tris(2,4-di-*t*-butylphenyl)phosphite proved to be large enough in terms of steric demand (*Tolman* cone angle) to stabilise the monosubstituted hydride under typical reaction conditions, but the reaction rate was too low for industrial hydroformylation. Current research is focused on modifications of steric and electronic properties of various phosphites to increase the rate of reaction. Further understanding of phosphite-modified Co-catalysed hydroformylation, as well as more-detailed kinetic investigations on factors influencing different steps in the catalytic cycle, are necessary.

Financial support from *Sasol* (including postdoctoral funding for *M. H.* and *R. M.*) and the *Research Funds* of the University of Johannesburg and the University of the Free State are gratefully acknowledged. Part of this material is based on work supported by the *South African National Research Foundation* (*SA NRF*) (GUN 2053397). Any opinion, findings, and conclusions or recommendations expressed in this material are those of the authors and do not necessarily reflect the views of the *SA NRF*. We thank Prof. *D. Levendis* and Dr. *D. Billing* (University of Johannesburg) for the use of their diffractometer, and Mr. *A. J. Muller* and Mr. *L. Kirsten* for data collection and assistance with structure analysis. We also acknowledge Mr. *K. Mokheseng* (*Sasol*) for GC analyses, and Mr. *J. A. Vorster* (University of Johannesburg) for assistance with HP-NMR experiments. We thank Prof. *M. J. Green*, Dr. *S. Otto*, Dr. *C. Grove*, and Dr. *C. Crause* (*Sasol*) for helpful discussions.

REFERENCES

[1] O. Roelen, Ger. Pat. 949 548, 1938.
[2] C. D. Frohning, C. W. Kohlpaintner, in 'Applied Homogeneous Catalysis with Organometallic Compounds', Eds. B. Cornils, W. A. Herrmann, VCH, Weinheim, 1996, Vol. 1, p. 29; P. W. N. M. van Leeuwen, 'Homogeneous Catalysis, Understanding the Art', Kluwer, Dordrecht, 2004.
[3] L. H. Slaugh, R. D. Mullineaux, U.S. Pat. 3.239.569, 1966.

[4] L. H. Slaugh, R. D. Mullineaux, U.S. Pat. 3.239.570, 1966.
[5] L. H. Slaugh, R. D. Mullineaux, *J. Organomet. Chem.* **1968**, *13*, 469.
[6] M. Beller, B. Cornils, C. D. Frohning, C. W. Kohlpainter, *J. Mol. Catal., A: Chem.* **1995**, *104*, 17.
[7] R. F. Heck, D. S. Breslow, *Chem. Ind. (London)* **1960**, 467; R. F. Heck, D. S. Breslow, *J. Am. Chem. Soc.* **1961**, *83*, 4023.
[8] J. P. Steynberg, K. Govender, P. J. Steynberg, WO Pat., 2002014248, 2002.
[9] C. Crause, L. Bennie, L. Damoense, C. L. Dwyer, C. Grove, N. Grimmer, W. Janse van Rensburg, M. M. Kirk, K. M. Mokheseng, S. Otto, P. J. Steynberg, *J. Chem. Soc., Dalton Trans.* **2003**, 2036.
[10] J. K. Merzweiler, H. M. Tenney, U.S. Pat. 3351666, 1967.
[11] M. Haumann, R. Meijboom, J. R. Moss, A. Roodt, *J. Chem. Soc., Dalton Trans.* **2004**, 1679.
[12] C. A. Tolman, *Chem. Rev.* **1977**, *77*, 313.
[13] D. F. Shriver, M. A. Drezdzon, 'The Manipulation of Air-Sensitive Compounds', Wiley-Interscience, New York, 1986.
[14] D. D. Perrin, W. L. F. Armarego, 'Purifiction of Laboratory Chemicals', Pergamon Press, Oxford, 1988.
[15] C. Loubscher, S. Lotz, *Inorg. Synth.* **1992**, *29*, 178.
[16] W. Rigby, R. Whyman, K. Wilding, *J. Phys. E.* **1970**, *3*, 572.
[17] S. Otto, A. Roodt, *Inorg. Chem. Commun.* **2001**, *49*, 4.
[18] SCIENTIST for Windows: Program for Least-Squares Parameter Estimation, Version 4.00, *Micromath Inc.*, Utah, 1990.
[19] D. C. Roe, *J. Magn. Res.* **1985**, *63*, 388; I. T. Horváth, J. M. Miller, *Chem. Rev.* **1991**, *91*, 1339.
[20] SAINT, *Siemens Analytical X-ray Instruments Inc.*, Madison, Wisconsin, USA, 1995.
[21] SADABS, *Siemens Analytical X-ray Instruments Inc.*, Madison, Wisconsin, USA.
[22] G. M. Sheldrick, SHELXL97, Program for solving crystal structures, University of Göttingen, Göttingen, Germany, 1997.
[23] K. Brandenburg, M. Berndt, DIAMOND, 1999, Version 2.1c, *Crystal Impact GbR*, Bonn, Germany.
[24] M. Datt, D. Foster, L. Bennie, C. Steenkamp, J. Huyser, L. Kirsten, G. Steyl, A. Roodt, R. Crous, *J. Chem. Soc., Dalton Trans.* **2005**, in preparation.
[25] D. Zhao, L. Brammer, *Inorg. Chem*. **1994**, *33*, 5897.
[26] T. Bartik, T. Krummeling, B. Happ, A. Sieker, L. Marko, R. Boese, R. Ugo, C. Zucchi, G. Palyi. *Catal. Lett*. **1993**, *19*, 383.
[27] J. S. Leigh, K. H. Whitmire, *Acta. Crystallogr., Sect. C* **1989**, *45*, 210.
[28] R. V. Gholap, O. M. Kut, J. R. Bourne, *Ind. Eng. Chem. Res.* **1992**, *31*, 1597.
[29] R. M. Desphande, R. V. Chaudhari, *J. Catal*. **1989**, *115*, 326.

Received November 14, 2004